Proceedings of the Seventh International Conference on
Railway Technology: Research, Development and Maintenance
Edited by: J. Pombo
Civil-Comp Conferences, Volume 15, Paper 5.8
Civil-Comp Press, Edinburgh, United Kingdom, 2026
ISSN: 2753-3239, doi: 10.4203/ccc.15.5.8


# A Study on the Aerodynamic Characteristics and Drag-Reduction Structural Optimisation of Inside-Axle-Box Bogies in High-Speed Trains

**D. Luo[1], T. Wang[1,2,3], Y. Wang[1] and Y. Feng[1,4]**

**[1]School of Traffic and Transportation Engineering, Central South University, Hunan, China**
**[2]College of Future Technology, Hunan University, China**
**[3]College of Mechanical and Vehicle Engineering, Hunan University, China**
**[4] CRRC Qingdao Sifang CO., LTD., Shandong, China**

## Abstract

The inside-axle-box bogie, as a novel bogie configuration, offers advantages in structural integration, spatial arrangement, and dynamic performance. However, its application to high-speed trains remains limited, and its aerodynamic characteristics and drag-reduction mechanisms are still unclear. Due to the complex geometry and exposed components in the bogie region, flow separation, local high-pressure concentration, and wake vortex evolution are easily induced, making this region a major source of underbody aerodynamic drag. In this study, a four-car high-speed train was investigated using models of the original bogie, a coupling fairing scheme, and a bottom fairing scheme. The aerodynamic drag, pressure field, and velocity field at different speeds were analysed to reveal the flow organisation and drag-reduction mechanisms in the inside-axle-box bogie region. The results showed that both fairing schemes improve the local flow structure, suppress flow separation and wake disturbance, and reduce the aerodynamic drag of both the bogie region and the entire train. The bottom fairing scheme exhibited more stable drag reduction, with a maximum drag-reduction rate of 12.4%. These findings provide provides theoretical support for the aerodynamic optimisation of high-speed trains with inside-axle-box bogies and the development of underbody drag-reduction structures.

**Keywords:** high-speed trains, inside-axle-box bogies, fairings, aerodynamic drag reduction, numerical simulation, aerodynamic optimisation.

# 1 Introduction

As the operating speeds of high-speed trains continue to increase, aerodynamic drag accounts for an ever-larger proportion of total energy consumption, making it a key factor affecting train performance and economic efficiency [1]. While the optimisation of the exterior shapes of the train's nose, tail, and pantographs has gradually matured, there remains significant room for drag reduction optimisation in the underbody region, where the complex geometry of the bogies tends to induce separation flows and large-scale vortex structures, thereby significantly increasing total drag [2]. While traditional bogies with external axle boxes meet structural strength and maintenance requirements, their discrete and exposed components make it difficult to further improve the underbody flow field characteristics, hindering efforts to achieve higher speed ratings and energy-saving targets [3]. As a new integrated configuration, the inside-axle-box bogies effectively reduces the adverse aerodynamic effects caused by local geometric discontinuities by relocating the axle box suspension mechanism from the outer side of the wheel to the inner side, thereby providing a new structural foundation for research on bogie aerodynamic drag reduction [4]. A systematic evaluation of the aerodynamic characteristics of this configuration and the optimisation potential of its drag-reduction structures is therefore of considerable engineering significance and research value for enhancing the aerodynamic performance of high-speed trains and promoting the integrated arrangement of underfloor components.

In recent years, scholars both domestically and internationally have conducted research on the aerodynamic characteristics of the bogie region. In investigating the airflow patterns beneath trains with and without bogies, Wang et al. [5] found that bogies significantly alter the wake structure at the rear of high-speed trains and enhance the slipstream effect, while Jonsson et al. [6] found that bogies markedly increase the velocity and velocity gradient of the flow field beneath the train. Liu et al. [7] found that bogies are a key factor influencing the generation and evolution of wake vortices and should not be neglected in experiments or numerical simulations; furthermore, the last bogie of the rear car can cause significant pulsations in the wake. Dong et al. [8] investigated the effects of simplified bogie geometry on the flow field and aerodynamic forces around a train, noting that simplifying the bogie significantly affects the underbody flow, near-wake flow, and local aerodynamic force distribution. Wang et al. [9] investigated different enclosure structures for bogies, and the results indicated that fully enclosed bogies can significantly reduce aerodynamic pressure fluctuations in the bogie region. GAO et al. [10] found that moving the bogie position backward by 1 m and 2 m, respectively, reduced the aerodynamic drag of the lead car by 7.75% and 10.56%, and the total drag of the three-car train by 5.57% and 6.58%. However, due to space constraints within the bogie compartment, the distance by which the bogie can be moved is also significantly limited. Wang et al. [11] investigated the effects of different bogie positions on train aerodynamic behaviour, noting that bogie position influences the development of the bottom boundary layer, wake structure, and overall aerodynamic forces. Overall, research on the aerodynamic characteristics of conventional bogie areas is relatively mature, whereas studies on inside-axle-box bogies remain insufficient. Nevertheless, the experience accumulated from existing research regarding flow mechanisms can still serve as a reference for studies on the aerodynamic performance of inside-axle-box bogies.

Regarding drag-reducing aerodynamic design for the bogie area, ZHANG et al. [12] developed a new composite bogie cutout configuration through numerical simulations and wind tunnel tests, achieving a 2.29% reduction in drag for a three-car train.LIU et al. [13] designed a bottom deflector and found that installing this deflector on the No. 1 bogie of the lead car alone could achieve an 11.99% reduction in drag across three cars. Zhang et al. [14] proposed installing diversion slots in the bogie area; by inducing local separation and suppressing the large-scale inflow of air into the bogie region, they achieved dual improvements in under-car flow and wake structure. Moon et al. [15] used the South Korean HEMU-430X high-speed train as the subject of their study and employed CFD methods to investigate the impact of different types of bogie fairings on the train's aerodynamic drag. The results showed that the use of a fully enclosed fairing in the bogie area resulted in the most significant reduction in aerodynamic drag, reaching 7.8%. Xie et al. [3] conducted design research on integrated bogie fairings, demonstrating that integrated fairings can further enhance drag reduction in the bogie area. Existing aerodynamic drag reduction designs for traditional bogie regions have established a relatively comprehensive body of technical approaches. Research findings in areas such as flow guidance, separation suppression, reduction of inflow intrusion, and optimisation of cavity flow can provide valuable guidance for the drag reduction structural design and aerodynamic optimisation of inside-axle-box bogies.

In this paper, the aerodynamic characteristics of inside-axle-box bogies are investigated, and their drag-reduction structures are optimised. Numerical simulation methods are employed to systematically analyze the flow patterns in the bogie region, revealing the primary forms of aerodynamic disturbance and sources of drag; Fairing-based drag-reduction schemes were designed for the coupling and underbody regions in order to investigate the influence of different configurations on flow separation and wake evolution, and to elucidate the underlying drag-reduction mechanisms from the perspective of flow dynamics. The research results provide a theoretical basis for improving the aerodynamic performance of inside-axle-box bogies and for designing underbody drag-reduction structures.

# 2 Computational Models and Methods

## 2.1 Computational model

As shown in Figure 1, this study employs a 1:8 scale model of a specific high-speed train [16]. The train consists of a four-car formation, with bogies featuring built-in axle boxes. Bogie components primarily include the frame, wheelsets, motors, centre pins, and air springs. Using the train height H (H = 4.11 m) as the characteristic length, the length of the lead and trailing cars is 6.46H, while the length of the intermediate cars is 6.35H. To improve the efficiency of numerical simulations, components that have a minor impact on the flow field around the train—particularly the flow field beneath the train—such as windows, headlights, and pantographs, were smoothed [17]. As the primary focus of this study, the bogie is modelled while retaining its key features but omitting its fine-scale internal structures [8]. For ease of reference, bogies are designated by their position within the train; for example, the bogie at the end of the second car is designated as Bogie 2-1.

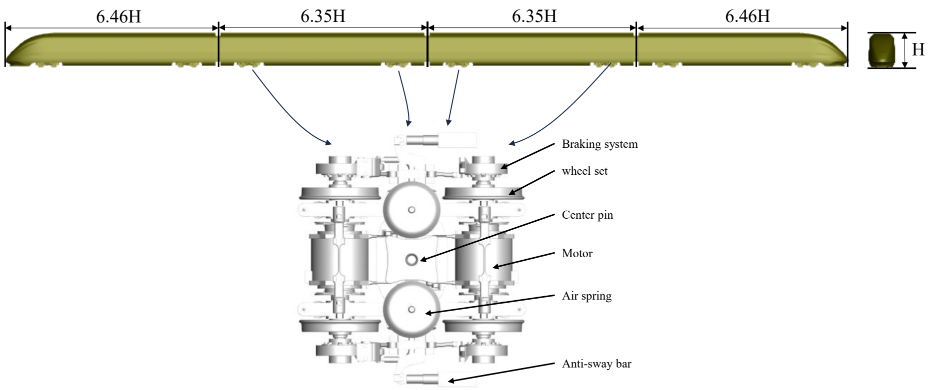


Figure 1: Train model.

To optimise the exposed key components of the original bogie, two groups of schemes are considered, as shown in Figure 2: coupling fairings (b1-b3) and bottom fairings (c1-c3). Schemes b1-b3 focus on aerodynamic shaping of the coupling region. Scheme b1 uses a circular fairing to remove sharp geometric discontinuities and weaken local separation. Scheme b2 replaces the circular fairing with an octagonal fairing that better matches the surrounding layout while maintaining compactness. Scheme b3 further narrows the octagonal form of b2, reducing frontal area while preserving structural continuity.

Schemes c1-c3 target the bogie underside, where complex components induce strong vortical structures. Scheme c1 adopts a curved fairing to guide the underbody flow more smoothly. Scheme c2 further adapts the fairing to the local geometry of the centre pin and tension torsion bar to improve continuity. Scheme c3 simplifies the underside with a planar fairing based on c1. Together, these two categories provide a clear basis for comparing aerodynamic performance and drag-reduction mechanisms.

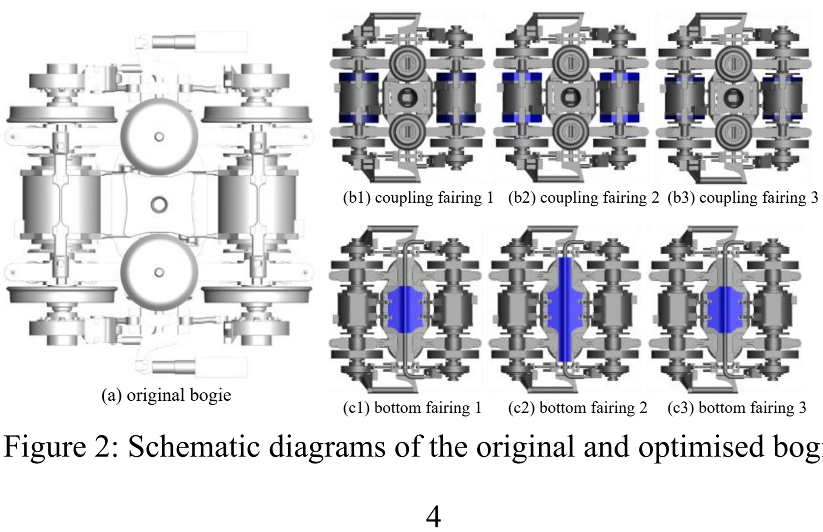


Figure 2: Schematic diagrams of the original and optimised bogies.

## 2.2 Computational Domain and Mesh Generation

To ensure sufficient flow development and to minimise boundary effects, a computational domain of 117 m x 78 m x 39.976 m is established, as shown in Figure 3. The inlet is placed 39 m upstream of the train. Under the incompressible-flow assumption, a velocity-inlet condition is imposed at the inlet and a pressure-outlet condition with zero gauge pressure is imposed at the outlet. Symmetry conditions are applied to the top and side boundaries. To represent the relative motion between the train, the wheelsets, and the ground, the ground and track are modelled as moving walls in the direction opposite to train travel.

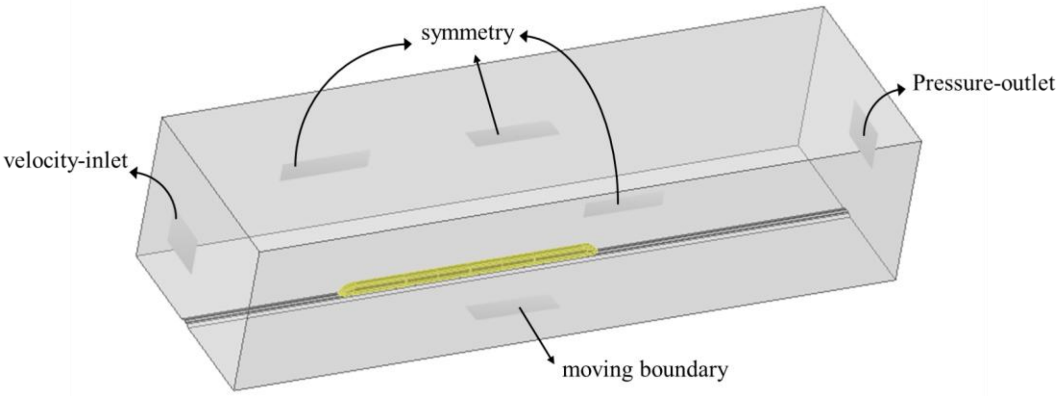


Figure 3: Computational Domain and Boundary Conditions.

Figure 4 shows the computational domain and details of the vehicle body mesh. The computational domain is discretized using a poly-hexcore mesh method, with multiple local refinements around the vehicle body and bogies. The wall-adjacent regions employ the wall function method. A total of 10 boundary layers are established on the model walls, with the first boundary layer set at a height of 2 mm, a mesh growth rate of 1.2, and a total of 24 million cells. The maximum face mesh size for the vehicle body is 40 mm, and the minimum is 20 mm; for the bogie, the maximum face mesh size is 10 mm, and the minimum is 3 mm; the maximum surface mesh size for the track is 400 mm, and the minimum is 40 mm; the maximum dimension of the bottom surface of the computational domain is 1900 mm. The volumetric mesh sizes are 400 mm and 100 mm, respectively. This study focuses on the bogie region, where a refined zone is also established to ensure that the y+ value remains around 1, thereby satisfying the wall function.

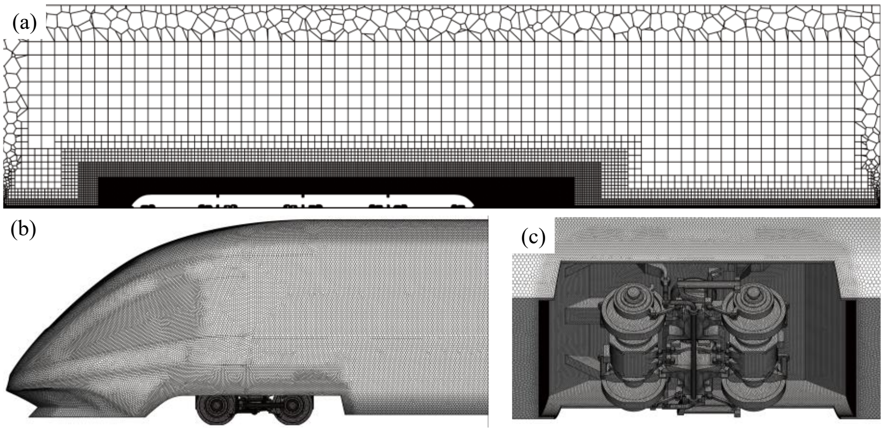


(a) Longitudinal section mesh distribution of the computational domain: (b) Car body surface mesh: (c) Bogie region mesh
Figure 4: Detailed mesh of the car body and bogie sections.

### 2.3 Solution Method

This paper investigates the aerodynamic characteristics of a 1:8 scale model of a high-speed train, with the governing equations solved based on the steady-state Reynolds-averaged Navier-Stokes equations. To reliably predict the complex flow characteristics in the bogie and axle box regions, the SST k-ω model was selected as the turbulence model. This model offers high resolution in the near-wall region, accurately describing boundary layer development, while maintaining good robustness in the free shear layer and demonstrating superior responsiveness to reverse pressure gradients and flow separation. Compared to traditional k-models, the SST k-ω model performs better in engineering flows involving high shear, separation, and reattachment; therefore, it is suitable for aerodynamic simulation requirements in the confined spaces inside high-speed train bogies. The control equations are discretized using the Finite Volume Method (FVM). The SIMPLEC algorithm is selected for the coupled pressure and velocity fields, and an iterative method is used to correct the pressure field. The convection-diffusion terms are discretized using a second-order upwind scheme, while the time derivatives are discretized using a first-order implicit method. The convergence criterion is based on the residual of the continuity equation being less than 10e-6 or the variation range of the monitored physical quantity being less than 1%, thereby ensuring computational accuracy.

### 2.4 Method Validation

Because mesh quality strongly affects numerical accuracy, especially in complex flow regions, a grid-independence study was conducted using coarse, medium, and fine meshes, as listed in Table 1. After all cases reached stable convergence, the relative error of total train drag between the coarse mesh (16,178,876 cells) and the fine mesh (59,521,368 cells) was 5.5%, whereas the error between the medium mesh (27,671,876 cells) and the fine mesh was only 1.3%. Considering both accuracy and computational cost, the medium mesh was adopted for the subsequent simulations.

| Grid size | Number of cells | Aerodynamic drag [N] |
|---|---|---|
| Coarse mesh | 16178876 | 130.3 |
| medium mesh | 27671876 | 121.3 |
| fine mesh | 59521368 | 123.1 |

Table 1: Verification of grid independence.

## 2.5 Validation of Numerical Methods

To verify the accuracy of the numerical method presented in this paper, the numerical results were compared with previous experimental data. Xia et al. [18] conducted wind tunnel tests on a 1:8 scale model of a specific vehicle; therefore, the numerical simulation strategy described in this paper was applied to this model to validate the reliability of the simulation method. As shown in Figure 5, the pressure coefficient results along the upper centreline of the head car indicate that the numerical calculation results agree well with the wind tunnel test results. The simulation data curve and the experimental data curve overlap closely, indicating that the numerical calculation results are reliable. The pressure coefficient is a dimensionless number used to describe the pressure distribution on the surface of an object in fluid mechanics. Its formula is:

$$Cp = \frac{p - p_\infty}{\frac{1}{2}\rho V_\infty^2} \tag{1}$$

Here, $C_p$ is the pressure coefficient; $p$ is the static pressure at the point of interest; $p_\infty$ is the independent static pressure far from any disturbances; $\rho$ is the fluid density; and $V_\infty$ is the independent flow velocity far from any disturbances, i.e., the on-stream velocity.

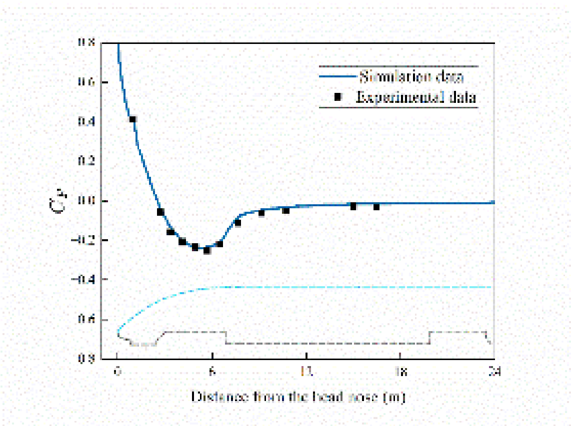


Figure 5: Comparison of pressure coefficient ($C_P$) along the upper centreline of the head car.

# 3 Results

This chapter focuses on the aerodynamic characteristics of the inside-axle-box bogie region. Through a systematic investigation of drag composition, pressure distribution, and velocity field structures, the flow mechanisms of the inboard bogie and the major adverse aerodynamic factors are revealed, thereby providing a basis for the subsequent proposal and performance evaluation of drag-reduction optimisation schemes for the bogie.

## 3.1 Comparison of Aerodynamic Drag

The trends in aerodynamic drag for different optimised configurations at various speed levels are shown in Tables 2 and 3. Overall, as the operating speed increases from 160 km/h to 400 km/h, aerodynamic drag increases significantly under all conditions, exhibiting a typical aerodynamic behaviour that scales with the square of the speed. At the same time, compared to the original configuration, all optimisation schemes achieved drag reductions to varying degrees, indicating that improving the flow organisation in the bogie area through structural modifications has a significant drag-reduction effect.

| Speed [km/h] | Original bogie [N] | Cupling encasement 1 [N] | Cupling encasement 2 [N] | Cupling encasement 3 [N] |
|---|---|---|---|---|
| 160 | 108.627 | 96.304 | 109.166 | 96.896 |
| 200 | 170.283 | 166.666 | 168.715 | 149.124 |
| 300 | 375.649 | 365.378 | 371.754 | 330.119 |
| 400 | 656.865 | 593.198 | 649.336 | 578.237 |

Table 2: Comparison of drag Under Optimised Conditions for Couplings.

| Speed [km/h] | Original bogie [N] | Bottom fairing 1 [N] | Bottom fairing 2 [N] | Bottom fairing 3 [N] |
|---|---|---|---|---|
| 160 | 108.627 | 96.543 | 96.802 | 96.035 |
| 200 | 170.283 | 149.875 | 149.077 | 149.313 |
| 300 | 375.649 | 331.269 | 329.082 | 330.337 |
| 400 | 656.865 | 593.198 | 581.281 | 579.312 |

Table 3: Comparison of drag Under Optimised Conditions for Couplings.

For the coupling fairings, the drag-reduction effect varies with speed. By smoothing geometric discontinuities in the coupling region, the fairings weaken local flow impingement and reduce pressure drag. Scheme b3 provides the most stable performance, achieving drag reductions of 12.1% and 12.0% at 300 and 400 km/h, respectively, because it balances structural continuity with a reduced frontal area. By contrast, Scheme b2 is less effective under some conditions, suggesting that its shape does not regulate the local flow path sufficiently.

The bottom fairings perform better overall than the coupling fairings. By streamlining the complex underside components, they improve near-ground flow continuity, weaken separation, and suppress wake turbulence. All three schemes provide stable drag reduction over the full speed range, and Schemes c2 and c3 achieve the best results at high speed, with a maximum drag-reduction rate of 12.4%.

Overall, the bottom-fairing schemes outperform the coupling-fairing schemes under most operating conditions. This indicates that the bogie underside dominates aerodynamic energy loss, whereas the coupling region mainly affects local flow organisation. The two approaches therefore act through different mechanisms: one reorganizes the overall underbody flow, and the other mitigates local geometric abruptness.

### 3.2 Pressure Field Analysis

Due to its complex structure and exposure to high-speed airflow beneath the train, the bogie area experiences localised airflow impact. When the airflow encounters protruding structures such as wheelsets and axle boxes at the front of the bogie, severe flow separation occurs. The intensity of this flow separation varies with different speed levels. Given that the aerodynamic drag generated by the train bogie shown in Figure 3-1 is significant, it is selected as the primary focus of this analysis. Pressure difference drag constitutes the major component of the aerodynamic drag generated by the entire bogie area; by analyzing the changes in surface pressure before and after optimisation, the drag-reduction mechanism of the optimised design can be elucidated.

As shown in Figure 6, the original bogie exhibits a pronounced high-pressure region near the anti-hunting damper (Zone 1), indicating direct flow impingement and substantial local pressure drag. In the rear side-beam region of the frame (Zone 2), alternating high- and low-pressure areas reflect evident separation and reattachment. In the bogie centre (Zone 3), strong low pressure and non-uniformity appear around the front and rear motors, showing that the internal flow is strongly disturbed by the complex geometry. After the coupling fairing is introduced, the high-pressure concentration in Zone 1 is weakened, the pressure gradient in Zone 2 is reduced, and the pressure distribution in Zone 3 becomes more uniform. These changes indicate that the fairing modifies the inflow path and suppresses local separation.

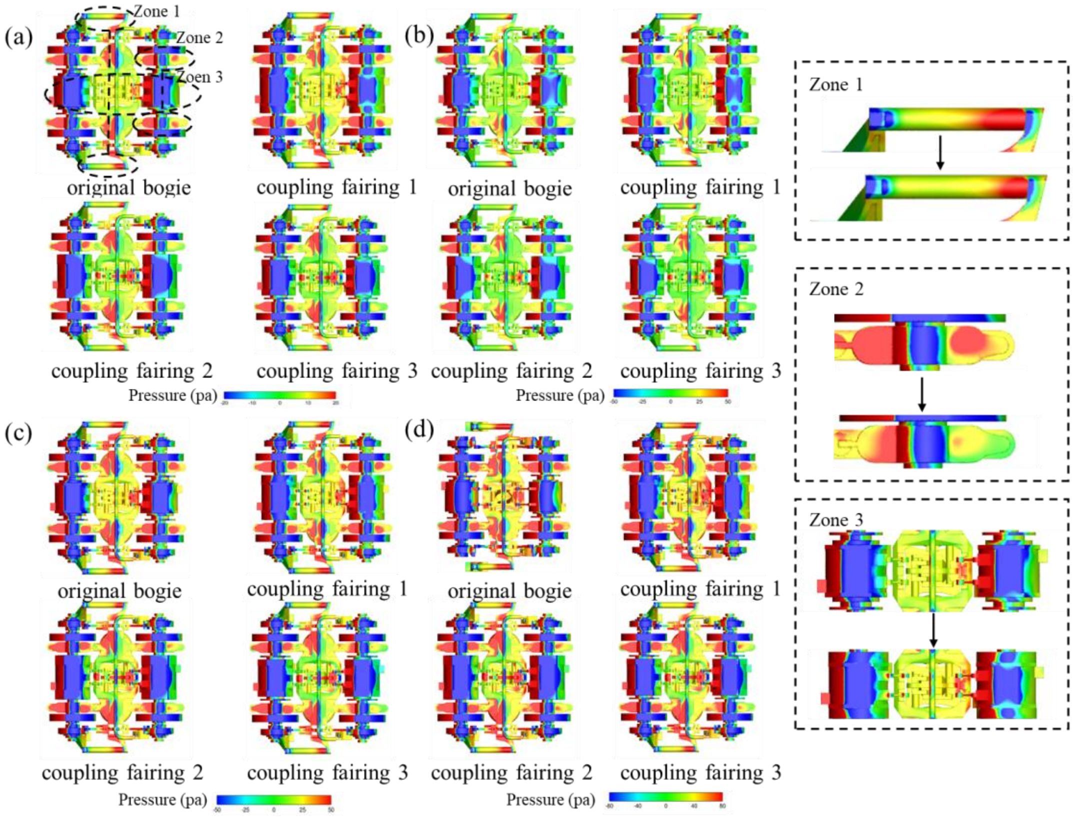


(a)160km/h (b)200km/h (c)300km/h (d)400km/h

Figure 6: Comparison of Bottom Views of the Pressure Flow Field Around the Bogie with an Optimised Coupling Design.

The bottom fairing configuration shown in Figure 7 has a more significant impact on the pressure field. In the original configuration, the complex bottom components cause multiple instances of flow separation as the airflow passes through this area, resulting in a strong high-pressure region on the windward side and a low-pressure wake region. After applying the bottom fairing, the bottom geometry is smoothed, allowing the airflow to pass continuously along the underside of the bogie. This effectively reduces the concentration of high pressure on the leading edge and diminishes the extent of the low-pressure region at the rear. Particularly in Fairing Schemes 2 and 3, the low-pressure region behind the bogie is significantly reduced, and the pressure distribution becomes more uniform, indicating that the wake structure has been effectively suppressed.

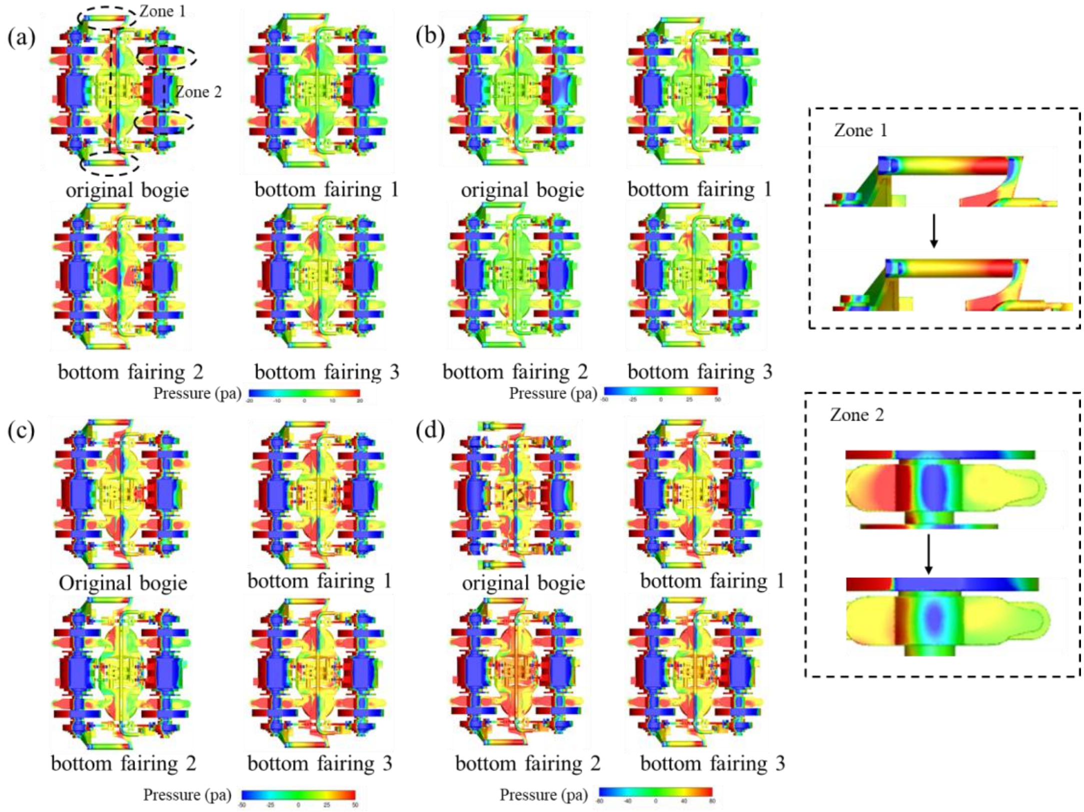


(a)160km/h (b)200km/h (c)300km/h (d)400km/h

Figure 6: Comparison of Bogie Pressure Flow Fields from the Bottom View for the Underbody Fairing Scheme.

### 3.3 Velocity Field Analysis

To further elucidate the flow structure characteristics in the bogie region, typical cross-sections (the coupling cross-section at Y = 0.043 m and the motor cross-section at Y = 0.93 m) were selected for analysis of the velocity field distribution. The velocity field distribution reflects the processes of acceleration, deceleration, and energy transfer of the airflow in the bogie region, and is of great significance for understanding flow separation and the formation of aerodynamic drag.

As shown in Figure 7, at the coupling cross-section, the original bogie forms relatively concentrated local high-speed zones (Zones 1 and 2) at the front ends of both the front and rear couplings, indicating that the oncoming flow undergoes significant compression and acceleration as it passes through these regions due to geometric constriction and structural abrupt changes. These localised high-speed zones not only intensify the airflow impact at the leading edge of the coupling but also cause a significant increase in the velocity gradient behind it, which can easily induce flow separation and the development of wake turbulence, thereby increasing energy loss. After installing the coupling fairing, the extent of the high-speed zones in Zones 1 and 2 was significantly reduced, and the high-speed core weakened. This indicates that the fairing mitigated the local geometric abrupt changes, allowing the airflow to transition smoothly before entering the coupling region, thereby reducing the degree of local acceleration and the velocity gradient. At the same time, the velocity distribution near the coupling became more uniform, and the flow line transitions were smoother, indicating that the flow structure was optimised, which helps suppress the development of subsequent separation.

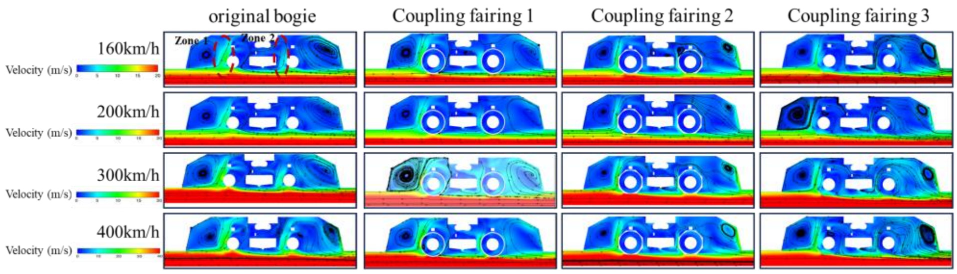

Figure 7: Comparison of velocity field slices at the bogie coupling section (Y = 0.043 m).

For the bottom-fairing configuration, the motor cross-section (Y = 0.093 m) was selected for analysis, as shown in Figure 8. In the original configuration, the high-speed airflow at the bottom is primarily concentrated near the ground; its upward and rearward extension is impeded by the complex structure, creating a localised low-speed stagnation zone behind the motor. This indicates significant flow separation and energy loss in this region. After installing the bottom fairing, the bottom geometric boundary was smoothed, enhancing the flow capacity as the airflow passes through the motor and its adjacent areas. The high-speed zone near Zone 1 expanded, while the low-speed stagnation zone was significantly reduced. This change indicates that the bottom fairing reduces flow obstruction, allowing more momentum to be transferred along the bottom of the bogie, thereby reducing the extent of flow separation. A comparison of different bottom-fairing schemes reveals that Schemes 2 and 3 exhibit a more uniform velocity distribution under high-speed conditions, with a smoother transition between the high-speed and low-speed zones. This indicates a more stable flow structure and reduced local shear stress, which helps minimise energy dissipation caused by velocity gradients.

In summary, the coupling fairing mainly reduces local acceleration and leading-edge separation in the coupling region, whereas the bottom fairing improves flow continuity and momentum transfer beneath the bogie. Both approaches improve the velocity-field organisation and thereby reduce aerodynamic drag.

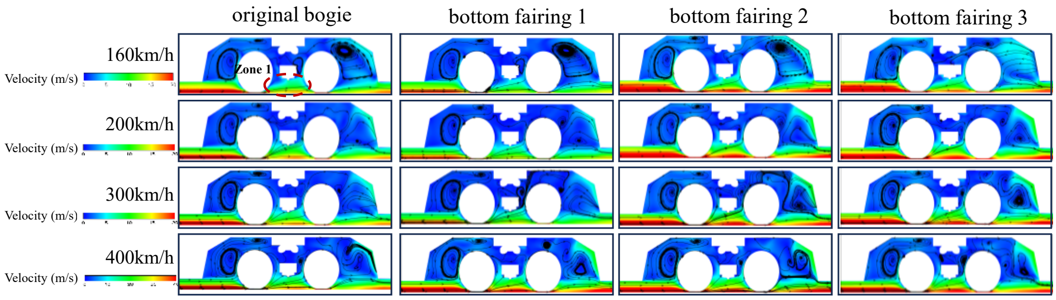

Figure 8: Comparison of velocity field slices at the bogie motor cross-section (Y = 0.093 m).

## 4 Conclusions and Contributions

(1) The aerodynamic drag in the area of the inside-axle-box bogie is primarily determined by the high-pressure shock zone induced by the front structure and the low-pressure wake zone formed by flow separation at the rear. As operating speed increases, both the pressure gradient and the velocity gradient increase in tandem, which is the main reason for the rapid rise in drag.

(2) The coupling fairing reduces local acceleration caused by geometric discontinuities, alleviates leading-edge high-pressure concentration and velocity gradients, and thus suppresses flow separation and local pressure drag; configurations with a better balance between structural continuity and frontal area show more stable drag-reduction performance. By contrast, the bottom fairing improves flow continuity, enhances momentum transfer, and weakens stagnation and wake regions, making it more effective for overall drag reduction, especially at high speeds, with a maximum drag reduction rate of 12.4%.

(3) The proposed fairing schemes improve the bogie flow field from different perspectives and provide a theoretical basis for aerodynamic optimisation of high-speed trains with inside-axle-box bogies as well as for the design of underbody drag-reduction structures.

## Acknowledgements

Authors acknowledges the financial support of the National Natural Science Foundation of China (Grant number 52322215, U24B20119& U2368213).

# References

[1] H.-q. Tian, "Review of research on high-speed railway aerodynamics in China", Transportation Safety and Environment, 1(1), 1-21, 2019.

[2] C. Jiang, J. Long, Y. Li, et al., "Numerical investigation on the aerodynamic drag reduction based on bottom deflectors and streamlined bogies of a high-speed train", Journal of Central South University, 31(9), 3312-3328, 2024.

[3] Z. Xie, W. Zeng, Y. Zhou, et al., "Aerodynamic drag reduction of high-speed trains via integrated bogie fairing designs", Railway Engineering Science, 1-19, 2026.

[4] S.C. Wu, Y.X. Liu, C.H. Li, et al., "On the fatigue performance and residual life of intercity railway axles with inside axle boxes", Engineering Fracture Mechanics, 197, 176-191, 2018.

[5] S. Wang, D. Burton, A. Herbst, et al., "The effect of bogies on high-speed train slipstream and wake", Journal of Fluids and Structures, 83, 471-489, 2018.

[6] M. Jönsson, C. Wagner, S. Loose, "Particle image velocimetry of the underfloor flow for generic high-speed train models in a water towing tank", Proceedings of the Institution of Mechanical Engineers, Part F: Journal of Rail and Rapid Transit, 228(2), 194-209, 2014.

[7] W. Liu, D. Guo, Z. Zhang, et al., "Effects of bogies on the wake flow of a high-speed train", Applied Sciences, 9(4), 759, 2019.

[8] T. Dong, X. Liang, S. Krajnović, et al., "Effects of simplifying train bogies on surrounding flow and aerodynamic forces", Journal of Wind Engineering and Industrial Aerodynamics, 191, 170-182, 2019.
[9] J. Wang, G. Minelli, T. Dong, et al., "The effect of bogie fairings on the slipstream and wake flow of a high-speed train. An IDDES study", Journal of Wind Engineering and Industrial Aerodynamics, 191, 183-202, 2019.
[10] G. Gao, F. Li, K. He, et al., "Investigation of bogie positions on the aerodynamic drag and near wake structure of a high-speed train", Journal of Wind Engineering and Industrial Aerodynamics, 185, 41-53, 2019.
[11] J. Wang, G. Minelli, X. Miao, et al., "The effect of bogie positions on the aerodynamic behaviour of a high-speed train: An IDDES study", Flow, Turbulence and Combustion, 107(2), 257-282, 2021.
[12] J. Zhang, J. Wang, Q. Wang, et al., "A study of the influence of bogie cut outs' angles on the aerodynamic performance of a high-speed train", Journal of Wind Engineering and Industrial Aerodynamics, 175, 153-168, 2018.
[13] W. Liu, Z. Ji, D. Guo, et al., "Effects of bottom deflectors on aerodynamic drag reduction of a high-speed train", Acta Mechanica Sinica, 38(5), 321251, 2022.
[14] J. Zhang, A. Adamu, F. Gidado, et al., "Flow control for aerodynamic drag reduction of a high-speed train with diversion slots on bogie regions", Physics of Fluids, 35(11), 2023.
[15] J.S. Moon, S.W. Kim, H.B. Kwon, "A study on the aerodynamic drag reduction of high-speed train using bogie side fairing", Journal of Computational Fluids Engineering, 19(1), 41-46, 2014.
[16] J. Niu, X. Liang, D. Zhou, "Experimental study on the effect of Reynolds number on aerodynamic performance of high-speed train with and without yaw angle", Journal of Wind Engineering and Industrial Aerodynamics, 157, 36-46, 2016.
[17] H. Hemida, "Contribution of computational wind engineering in train aerodynamics—past and future", Journal of Wind Engineering and Industrial Aerodynamics, 234, 105352, 2023.
[18] C. Xia, H. Wang, X. Shan, et al., "Effects of ground configurations on the slipstream and near wake of a high-speed train", Journal of Wind Engineering and Industrial Aerodynamics, 168, 177-189, 2017.